



# Applicable equivalent bow imperfections in GMNIA for Eurocode buckling curves – SHS, RHS and welded box sections

B. Somodi<sup>\*</sup>, E. Bärnkopf, B. Kövesdi

Department of Structural Engineering, Faculty of Civil Engineering, Budapest University of Technology and Economics, Műegyetem rkp. 3., H-1111 Budapest, Hungary

## ARTICLE INFO

### Keywords:

Flexural buckling  
GMNIA  
Closed section  
Equivalent imperfection  
High strength steel

## ABSTRACT

The direct resistance check using advanced numerical models is spreading among designers nowadays. Therefore, the development of accurate and up-to-date design rules supporting the FEM-based design of slender steel structures is an important task and prospective research field. Using the direct resistance check, the load carrying capacity of the steel structure under investigation is obtained as a result of geometrical and material nonlinear analysis using imperfections (GMNIA). The present paper investigates the imperfection magnitudes of slender steel columns and specifies the accurate value of the equivalent geometric imperfection to be applied for welded square, cold-formed and hot-rolled square (with rounded corners), and rectangular sections. Using the proposed imperfection magnitude, the load carrying capacities can be determined by GMNI analysis and the obtained results will be identical or very close to the buckling resistances calculated by the buckling curves of the Eurocode. The developed imperfection magnitude is given in closed form as a function of relative slenderness, steel strength and buckling curve parameter (imperfection factor  $\alpha$ ). Details on the determination of the necessary equivalent geometric imperfection and the obtained trends on the flexural buckling resistance are presented in the current paper.

## 1. Introduction

In civil engineering practice, defects in the fabrication of steel structures and the assembly of structural systems inevitably occur. The bearing capacity of structural elements subjected to compression is sensitive to imperfections, and it is important to take these unfavourable effects into account in the design. By imperfections in structural elements, it is meant both geometrical imperfections and residual stresses. Typically, the stability resistance of compressed elements can be determined using the buckling curves according to EN 1993-1-1 [1], which can be used to consider the effects of imperfections by selecting the appropriate curves. The use of buckling curves and element-by-element verification can be avoided if buckling verification is performed directly using advanced finite element modelling. This, however, requires that imperfections are to be considered in a second-order geometric and material nonlinear analysis (GMNIA). In contrast to a geometric nonlinear (GNI) analysis, GMNI analysis incorporates material nonlinearity in addition to geometric nonlinearity, and thus allows accurate prediction of the overall load-deformation response of the structure. However, the disadvantage of GMNI analysis is its higher

computational demand, but with the advances in computational power and software, designing with GMNIA is becoming more common in practice and is receiving increasing attention in research [2–9].

The magnitude of the initial imperfection to be considered in a design calculation depends on several aspects: (i) the reference resistance, which is considered to be a safe ultimate load, (ii) the type of analysis (GNI or GMNI), (iii) the failure criterion and (iv) whether geometric imperfection and residual stresses are modelled separately, or both are considered together by equivalent geometric imperfections. The imperfections of the structural elements can be taken into account in the modelling by modifying the perfect geometry or by using an equivalent horizontal force system. The residual stress pattern of steel structures depends on many factors [10,11], so direct modelling of residual stresses is usually too challenging for a general designer. Hence, for the determination of the standard load capacity, it is recommended to use the equivalent geometric imperfection that implicitly takes into account the combined effect of geometric and material (residual stress) imperfections. These applicable equivalent imperfections are defined in EN 1993-1-5 [12], but they only apply to geometric nonlinear (GNI) analysis, not to GMNI analysis. In the present paper we deal with their

<sup>\*</sup> Corresponding author.

E-mail address: [somodi.balazs@emk.bme.hu](mailto:somodi.balazs@emk.bme.hu) (B. Somodi).

definition, when applied to GMNI analysis.

The question arises as to whether the magnitude of the imperfections taken into account in the design calculations should be based on the manufacturing tolerances defined by the standards of EN 1090-2 [13] and EN 1993-1-5 [12], or whether a value should be defined that can be used to calculate statistically proven load capacities that model the resistances expected in reality with sufficient certainty and accuracy. The buckling curves according to EN 1993-1-1 are based on the Ayrton-Perry formula [14,15] and their current form is supported by extensive experimental and numerical data [16–23]. For this reason, the load capacities according to the EN 1993-1-1 deflection curves are considered as the standardized resistances for flexural buckling since decades until today. Therefore, these values are taken as the target result for the development of the appropriate imperfection magnitude, as is the case for the forthcoming revision of prEN 1993-1-1 [24]. Taking all these considerations into account, in this paper, for welded, cold-formed and hot-rolled square closed cross-section and welded rectangular box-sections, the magnitude of the equivalent imperfections to be used in the GMNI analysis is determined.

## 2. Literature review and research aim

The most common approaches to consider the effects of initial geometric imperfections in advanced analysis are (i) the modelling of imperfections by modifying the perfect shapes of the structural members modelled, (ii) the reduction of member stiffness, (iii) adoption of notional horizontal forces, or (iv) superposition of scaled elastic buckling modes [25]. The first approach is not practical for everyday engineering practice; therefore, it is not commonly used for the daily design. The stiffness reduction method has the advantage it does not require an explicit modelling of the imperfections. Therefore, several stiffness-reduction factors have been developed in the past to account for the effect of initial geometric imperfections [26–28]. The horizontal force method is widely used and has been adopted in different codes [29–34], since it allows modelling structures in their theoretically perfect configuration and applies a set of equivalent horizontal forces to consider the effect of the imperfections which forces are easy to apply in the daily design. Using advanced numerical modelling-based design, usually, the scaled shape of the elastic buckling mode is used as equivalent geometric imperfection, which approach assumes the first eigenmode represents the most critical imperfection [34]. This approach is also supported by many commercial software, which have the capabilities to convert the shape of the structure according to the selected eigenmodes or eigenmode combinations. However, it is known, the actual failure mode of the structure may be different from the first buckling mode due to the significant plastic deformations and load redistribution occurring in advanced analysis. Therefore, [35] recommends including additional higher order eigenmodes when incorporating initial geometric imperfections.

With improvements in computational power and software, design by GMNIA is becoming more widespread in practice and is receiving a growing level of attention in research [2–8]. Suitable and accurate equivalent bow imperfections by advanced GMNI analysis are therefore needed for design purposes. Currently, if designers design a structure using GMNI analysis, the magnitude and the shape of the applicable equivalent imperfection is defined by Annex C of EN 1993-1-5 [12] and Table 5.1. of EN1993-1-1 [1]. However, the application of these imperfections does not result the same value of resistance and same reliability level as the resistance obtained from the flexural buckling curves of EN1993-1-1 [1]. The tabulated approach developed in [36,37] and applied in EN 1993-1-1 [1] generally yields upper bound values of equivalent bow imperfections relative to the back-calculated values, resulting in safe-sided predictions of buckling resistance. But these imperfection magnitudes are developed for GNI analysis and not for GMNI analysis. Walport et al. [9] examined this issue in recent years. They observed that these imperfections are appropriate for use in design

by second order elastic analysis, their use in design by second order inelastic analysis is not generally appropriate and can lead to both unsafe and overly conservative resistance predictions depending in particular on the shape and material properties of the examined cross-section. Following calibration against benchmark FE ultimate loads, they provided a generally applicable imperfection magnitude for GMNI analysis, defined by Eq. (1), where  $\alpha$  is the imperfection factor for the relevant buckling curve as prescribed in EN1993-1-1 [1].

$$\frac{e_0}{L} = \frac{\alpha}{150} \quad (1)$$

The proposed equation is determined based on benchmark ultimate loads that are obtained from FE analysis using beam elements with geometric imperfections of amplitude  $L/1000$  and residual stresses. The proposed equivalent geometric imperfection can be used for several steel grades and stainless steel and applicable for different cross-section types. The varying influence of residual stresses for different cross-sections and axes of buckling is captured through the imperfection factor  $\alpha$ , which is determined according to the buckling curves prescribed in the different codes. However, it was observed that there is quite large scatter in the accurate applicable equivalent imperfections depending on slenderness, steel grade and cross-section geometry. The proposed equivalent imperfection is a general (average) value that can be used safely for all the examined cases.

The current research is intended to supplement and extend the research results of Walport et al. [9]. Our main aim is to complement the results already obtained by creating a method using the characteristic value of the buckling resistance as target values. We have chosen the Eurocode-based buckling curves as target values, which present the standardized characteristic buckling resistance, and we determine the necessary equivalent geometric imperfections depending on the relative slenderness ratio. We believe that both methods have their merits. For design purposes, designer can use the general recommendation of Walport et al. (or the average imperfection factor based on our current investigations), that is good for all sections and sufficiently accurate. However, in the case where the designer wants to further optimise a resistance calculation method, or in the case of mass production, where small material savings can result in large cost savings, the designer could have the possibility to use a more accurate design procedure using the slenderness dependent imperfection magnitudes. The new approach can be applied specifically for one section type, but it can be used to obtain more favourable load bearing capacities. Therefore, in the current paper our research aim is to determine the accurate applicable equivalent imperfection magnitude for welded square and rectangular box-sections and for cold-formed and hot-rolled SHS and RHS section columns made of carbon steel. In present paper, not the previously mentioned benchmark load capacity is considered as the target resistance, but the load capacity according to the EN 1993-1-1 currently in force. Our motivation is that it is wanted to provide an applicable suggestion for the value of the equivalent imperfection to be used in GMNI analysis for practicing design engineers, which would provide close resistance to the analytically calculated buckling resistance values. This approach is not the most accurate evaluation approach, because it does not consider the accurate buckling resistance of the analysed columns and it is not based on own statistical evaluation. But the application of the developed equivalent geometric imperfection leads to similar buckling resistance than the Eurocode-based buckling curves, and it provides similar accuracy than the standardized load capacity. Using the currently proposed imperfection magnitudes, the calculated buckling resistances will be identical to the resistance provided by EN1993-1-1 [1] using buckling curves. For this reason, although the analysed phenomenon is a non-deterministic phenomenon for which the expected load capacity can only be “accurately” determined in a stochastic way, nevertheless, since the goal in our case is to obtain the current load capacity value using FEM, it can be treated as a well-defined deterministic target value and the analysis can be performed in a deterministic way, obtaining the

exact equivalent imperfection that will give the standard manual design load capacity value using FEM.

In the current paper it is also analysed how the cross-section geometry and steel grade affect the applicable equivalent geometric imperfection to be applied in GMNI analysis. Based on the current research findings, new design equation is proposed to obtain the applicable equivalent imperfection magnitude in function of the relative slenderness ratio ( $\lambda$ ), steel grade and cross-section geometry for square box-section columns. Then, by modifying the formula developed for welded square section columns, proposals are made for cold-formed and hot-rolled square hollow and welded rectangular section columns. For hollow section columns, sections with rounded corner zones are tested and the differences resulting from this geometrical variation are studied and evaluated.

### 3. Research strategy

To evaluate the applicable amplitude of the equivalent geometric imperfection, numerical calculations are carried out varying the applied imperfection magnitude using an iteration process. In the present paper instead of the imperfection amplitude ( $e_{glob}$ ) always the ratio  $L/e_{glob}$  is analysed, which is called as imperfection amplifier ( $k_{globimp}$ ). The relevant resistance value according to EN1993-1-1 [1] is calculated ( $R_{EC}$ ) and considered as benchmark target resistance. This resistance value is chosen as a target value because it gives accurate and statistically validated resistances fitting the safety requirements of EN 1990 [38]. EN1993-1-1 defines five different buckling curves (a0, a-d), the choice of which should be used is based on the cross-section type, the manufacturing process, and the buckling plane. In the current research applicable equivalent geometric imperfections are defined for all the different buckling curves (in function of the  $\alpha$  imperfection parameter), therefore the proposed equations have a general applicability. All the effect coming from the manufacturing process and the supporting condition can be considered by the selection of the buckling curve (it means, by changing the  $\alpha$  parameter in the imperfection magnitude calculation). The target buckling resistance gave the goal of the iteration process to ensure the same buckling resistance determined using the numerical model than provided by the standard design process. The equality of these two values ensures the application of GMNI analysis provides the same accuracy and safety margin as the current standard design method based on hand calculations. One example for the imperfection sensitivity study and on the determination strategy of the necessary equivalent geometric imperfection can be seen in Fig. 1. The horizontal axis shows the applied imperfection amplifier factors and the vertical axis presents the flexural buckling resistance. The target buckling resistance calculated from the Eurocode-based buckling curve for this particular case is shown by horizontal line. Based on the intersection

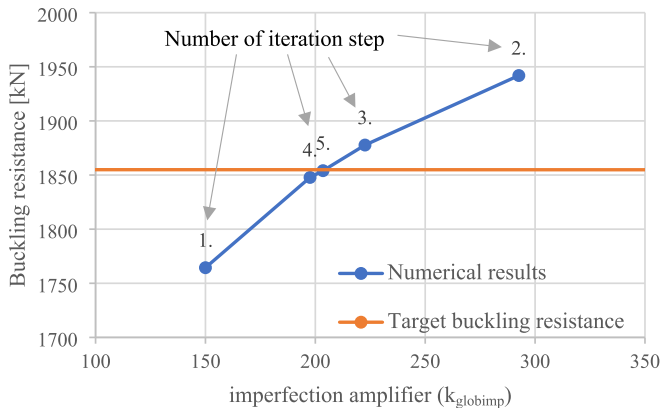


Fig. 1. Results of imperfection sensitivity study and determination of necessary imperfection amplifier factor.

point of the target buckling resistance and the imperfection sensitivity study, the necessary imperfection magnitude is determined. A similar sensitivity study has been executed to all analysed cross-section geometries and steel grades.

An automatic calculation and evaluation process has been developed to find the required intersection point. During the iteration process, after each numerical calculation the obtained resistance is determined as  $R_{num,i}$ , where the applied equivalent imperfection is  $e_{glob,i}$ , therefore the applied imperfection amplifier is  $k_{globimp,i}$ . For the next iteration process  $k_{globimp}$  is calculated based on Eq. (2).

$$k_{globimp,i+1} = k_{globimp,i} - \frac{R_{num,i} - R_{EC}}{R_{num,i} - R_{num,i-1}} (k_{globimp,i} - k_{globimp,i-1}) \quad (2)$$

For each analysed case always at least three iteration step is calculated, and the iteration process is stopped if the error in the resistance was smaller than 1% for the last two iteration step, see Eq. (3).

$$\left| \frac{R_{num,i-1}}{R_{EC}} - 1 \right| < 1\% \text{ and } \left| \frac{R_{num,i}}{R_{EC}} - 1 \right| < 1\% \quad (3)$$

If the criteria of Eq. (3) is met,  $k_{globimp,i+1}$  is calculated according to Eq. (2) and considered as the final value of the necessary imperfection amplifier. Therefore, using the obtained equivalent imperfection in GMNI analysis, the target resistance is reached with an accuracy of  $<1\%$ . Because of the extra iteration step, the final accuracy was generally around 0,1%.

In the numerical parametric study compressed columns having different cross-section geometry and different steel grades are examined. For each studied combination of geometry and steel grade the above-mentioned iteration process is executed for the five different buckling curves of EN1993-1-1 [1] and for 10 different global slenderness values, as summarised in Table 1. It means, a total of 50 imperfection amplifiers ( $k_{globimp}$ ) are determined to each examined combination of geometry and steel grade. Relative slenderness can be calculated according to Eq. (4).

$$\lambda = \frac{L_{cr}}{i} \times \frac{1}{93.9\epsilon} \text{ where } \epsilon = \sqrt{\frac{235}{f_y}}, \quad (4)$$

where  $L_{cr}$  is the buckling length,  $i$  is the radius of gyration,  $f_y$  is the yield strength.

Using the numerically obtained necessary equivalent imperfections closed functions are created to estimate the applicable imperfection amplifier. These are presented in detail in the next chapters. In order to check the appropriateness of the generated estimation functions, the resistance values are back-calculated using the equivalent imperfections calculated from the closed functions. These resistance values are noted by  $R_{XY}$ . The relative error of a proposed equivalent imperfection function is calculated according to Eq. (5).

$$\delta = \frac{R_{XY}}{R_{EC}} - 1 \quad (5)$$

Table 1  
Investigated cases for each type of columns.

	Relative global slenderness ( $\lambda$ )	Buckling curve (imperfection factor $\alpha$ )
Number of cases	10	5
	0.30	a <sub>0</sub> (0.13)
	0.35	a (0.21)
	0.50	b (0.34)
	0.65	c (0.49)
	0.80	d (0.76)
	1.00	
	1.20	
	1.50	
	1.80	
	2.00	

For a certain type of examined column (with given geometry and steel grade) there are 50 different cases according to Table 1, for these 50 cases 50 different relative errors  $\delta$  are calculated. In order to evaluate the appropriateness of the proposed function for the entire range of slenderness and for all the buckling curves, the maximum and the root-mean-square (RMS) of the 50 relative errors  $\delta$  are calculated, and these values are used to compare and evaluate the accuracy of the proposed equivalent imperfection functions.

#### 4. Numerical model development

##### 4.1. Geometric model, boundary conditions

The numerical model is developed using the finite element software Ansys 19.2 [39]. The model is a full shell model using four node thin shell elements (Shell 181). The load carrying capacities are determined by geometrical and material nonlinear analysis using equivalent geometric imperfections (including initial geometric imperfections and residual stresses). The applied finite element mesh size is verified by checking the appropriateness of the mathematical and geometrical finitization. The finite element mesh used, divides each side of the model into at least 16 parts in the transverse direction, in the longitudinal direction the size of the finite elements is double their transversal size. In mesh sensitivity analysis, several types of FE meshes, and element types are investigated. Fig. 2 illustrates one analysis used to check the effect of the number of longitudinal divisions of the section. In the figure, the ratio of the transverse divisions to the longitudinal divisions is 1 for case #1, 1.5 for case #2 and 2 for case #3.

The numerical model used in the present paper represents a simply supported box-section column subjected to concentrated force at the two ends. The developed model is shown in Fig. 3 with the applied finite element mesh, boundary and loading conditions.

##### 4.2. Material model

For the nonlinear calculations, a multilinear material model is used according to the proposal of Gardner et al. [8,40]; shown in Fig. 4. This multilinear material model can be defined from three basic parameters - elastic modulus ( $E$ ), yield strength ( $f_y$ ), and tensile strength ( $f_u$ ). The same material model is used in [9].

Nowadays, the application of high strength steels (HSS) is growing in civil engineering practice due to their numerous advantages. For this reason, high strength steels have been used in addition to testing of normal strength steel (NSS) columns. In the research program six different steel grades are used, namely: S235, S355, S460, S500, S700, S960. Originally, it is known that high-strength steels behave differently than columns made of normal strength steel; the linear behaviour of the stress-strain relationship ends before the yield strength is reached and

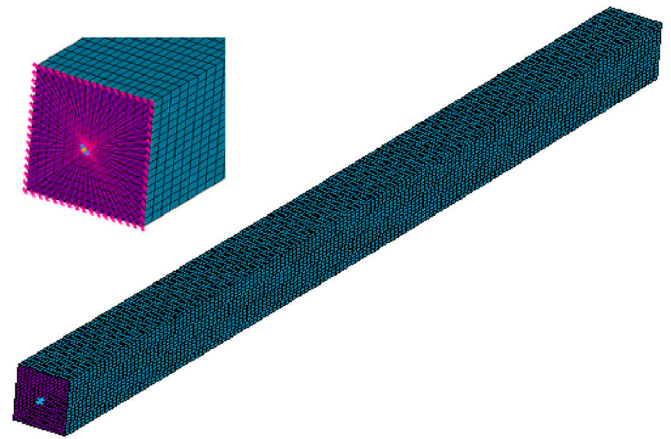


Fig. 3. Finite element model (mesh, boundary and loading conditions).

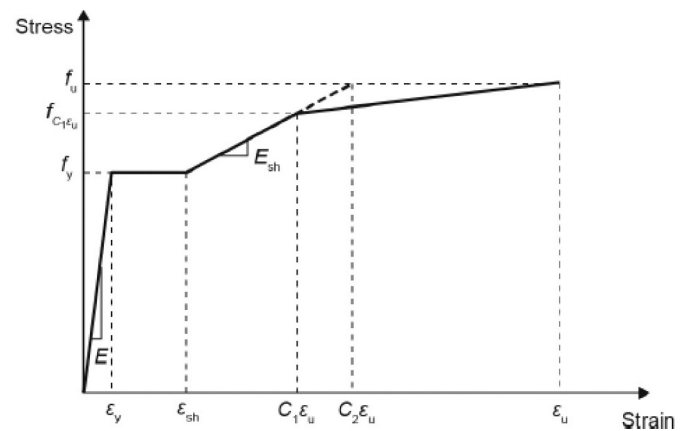


Fig. 4. Multilinear material model according to Gardner et al. [8,40].

even there is no yield plateau [41]. However, numerous recent studies show stress-strain curve of HSS steel grades can be similar than usual steel grades [42–45] depending on its manufacturing technique up to S700. Therefore, in the present study the material model shown in Fig. 4 is applied for all studied steel grades. To investigate high strength steel having Ramberg-Osgood-type material model are studied separately, their results are presented in a different paper.

##### 4.3. Applied equivalent geometrical imperfections

In the numerical model both the global and local imperfections are modelled using manually defined imperfection shapes. The global imperfection has a half-sine wave shape. The shape of the local imperfection is a continuous sine wave on each side of the specimen. The number of half-waves is equal to the rounded ratio of  $L/b$ , where  $L$  is the length of the column and  $b$  is the width of the cross-section. The amplitude of the global imperfection ( $e_{glob}$ ) is examined in present research, the global imperfection amplitude is commonly defined as the length divided by a certain constant ( $L/k_{globimp}$ ). In the current study the  $L/e_{glob} = k_{globimp}$ , named as imperfection amplifier is calculated for each case and the determined values are evaluated. The amplitude of the local imperfection is set to  $b/10000$ , where  $b$  is the width of the cross-section. Within the current paper, the pure flexural buckling resistance is investigated, therefore the amplitude of the local imperfection is set to a small value since the current study investigates only cross-sections belonging to cross-section classes 1–3, which are not sensitive to local plate buckling. Class 4 cross-sections need special treatment because interaction failure mode of local and global buckling. That problem is

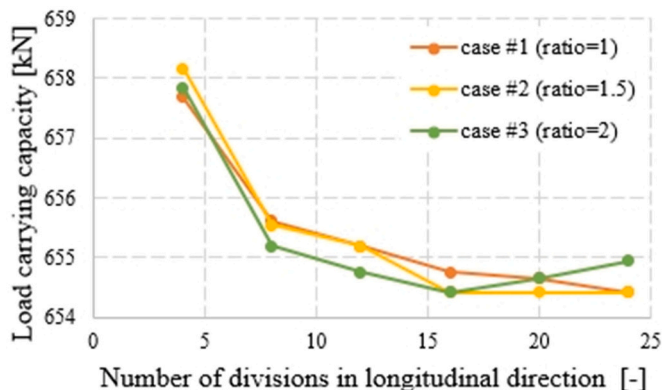


Fig. 2. Verification: determining the required mesh size.



analysed in a separate paper.

#### 4.4. Validation of numerical model

The finite element model was validated by comparison of the numerical simulation results to experimental data. The validation process is executed based on the test program executed by Somodi and Kövesdi, details are published in [46]. A typical load-deformation curve showing the comparison of the experimental results and numerical calculation is presented in Fig. 5. The comparison proves the accuracy of the numerical model. The stiffness, the structural behaviour and the ultimate load, all of them show good agreement with the test results.

### 5. Investigation of welded square box section

#### 5.1. Effect of cross-section dimensions on the bow imperfection

Welded box-section columns having seven different cross-sections built up from S355 steel grade are investigated at first to determine the required equivalent buckling imperfections for each buckling curve. The following variants are studied: (i) the basic case 250x250x8 cross-section, (ii) the  $b/t$  ratio does not change, but parameters  $b$  and  $t$  doubled or halved, (iii) only  $b$  or  $t$  changed, (iv) both parameters and  $b/t$  ratio also changed. Special attention is paid to testing columns having cross-section classes only 1, 2 and 3, because class 4 cross-sections need special treatment because interaction failure mode of local and global buckling. The studied cross-sections are summarised in Table 2. For each type of cross-section, 10 slenderness ratios (the relative slenderness varied between 0.3 and 2.2) are investigated by applying different span lengths and for each one the required equivalent bow imperfection is determined to obtain the same load carrying capacity as by using the corresponding buckling curves of EN1993-1-1 [1]. Fig. 6 presents the results of the study. The vertical axis shows the ratio between the required equivalent bow imperfection magnitude and the length of the element – imperfection amplifier ( $L/e_{glob} = k_{globimp}$ ), and the horizontal axis represents the relative global slenderness ratio of the analysed girders.

It can be seen, for the buckling curves of  $a_0$ ,  $a$ ,  $b$ ,  $c$  and  $d$ , the results fall approximately on a single curve (one curve for each) regardless of the geometry of the cross-section. It is found that all the results are within 2% of the average of the different cross-section results, therefore it can be concluded that for all square cross-sections the same imperfection amplifier  $k_{globimp}$  should be applied regardless of the thickness, width and  $b/t$  ratio. The diagram shows different imperfection amplifier curves belong to the different buckling curves. However, it is observed the difference between the curves can be described by the imperfection

factor  $\alpha$  given by EN1993-1-1 [1]. Fig. 7 shows all the imperfection amplifier curves multiplied by the imperfection factor  $\alpha$  for a single section. It is found that all the previous curves are close to each other and can be described by a single function that depends only the relative slenderness.

It is found Eq. (6) is a good approximation for the numerically obtained imperfection amplifier ( $k_{globimp}$ ), where  $A = -3.64$ ,  $B = 18.16$ ,  $C = 132$ ,  $\alpha$  is the imperfection factor and  $\lambda$  is relative slenderness.

$$k_{globimp,S355} = (\lambda_{rel}^A - B\lambda_{rel} + C)/\alpha \quad (6)$$

#### 5.2. Effect of steel grade on the required equivalent bow imperfection

Since the modification of the cross-section has no effect on the required equivalent bow imperfection, only one type of cross-section is tested for different steel grades. Six steel grades are studied: S235, S355, S460, S500, S700, S960, details are given in Table 3. The geometric dimensions of the sections are chosen so as all sections belong to cross-section class 3 or lower. The results of the numerical simulations are shown in Fig. 8.

For different steel grades, the same type of parallel curves is obtained for each buckling curve. The curve corresponding to the required equivalent bow imperfection is drawn highest for grade S235 and lowest for grade S960. In other words, for higher material grades, a lower imperfection amplifier, so higher equivalent geometric imperfection is required to achieve the same load carrying capacity. It is not in contradiction with previous research results showing high strength steel columns have larger buckling strength, because this study is for the calibration of the equivalent geometric imperfections, and for columns made of high strength steel different buckling curves can be used, leading to different or smaller required imperfection values.

It is also found Eq. (6) can be accurately applied for all the examined steel grades but with slightly different  $A$ ,  $B$  and  $C$  constants. The applicable constants are summarised in Table 4.

Fig. 9 shows the applied imperfection amplifier functions based on Eq. (6) multiplied by the imperfection factor  $\alpha$  for each examined steel grades (lines) and all the calculated numerical results (points), also multiplied by the imperfection factor  $\alpha$ .

Results show the curves presented in Fig. 9 have similar shape, and their difference can be described by the coefficient  $\varepsilon = \sqrt{(235/f_y)}$ . Fig. 10 shows all the data points and curves presented in Fig. 9, but the vertical axis now represents the imperfection amplifier  $k_{globimp}$  multiplied by the imperfection factor  $\alpha$  and divided by the coefficient  $\varepsilon$ . The results show that the imperfection amplifier  $k_{globimp}$  depends linearly on the coefficient  $\varepsilon$  with a good approximation.

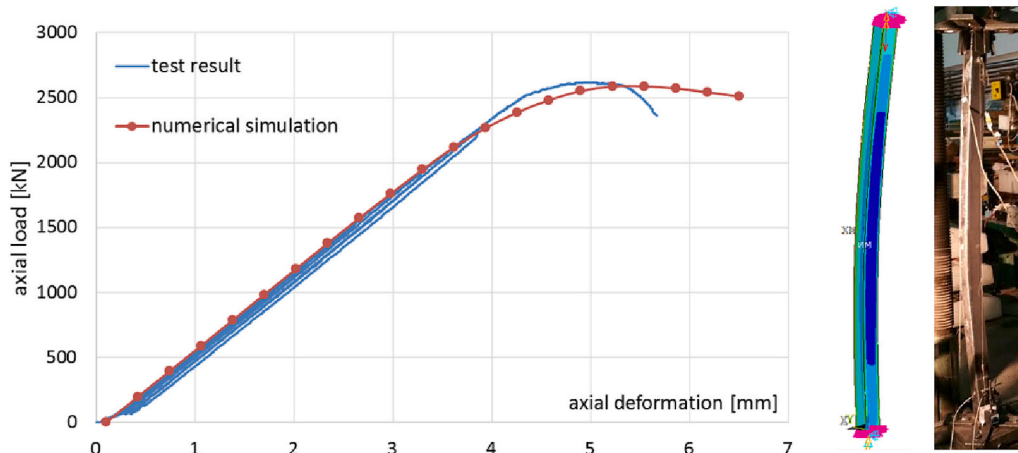
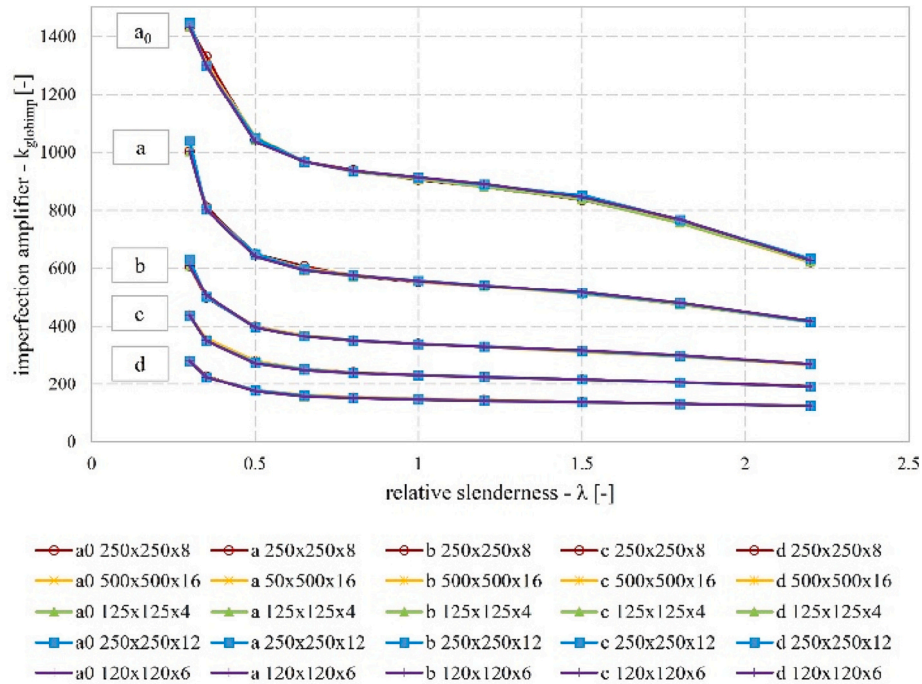


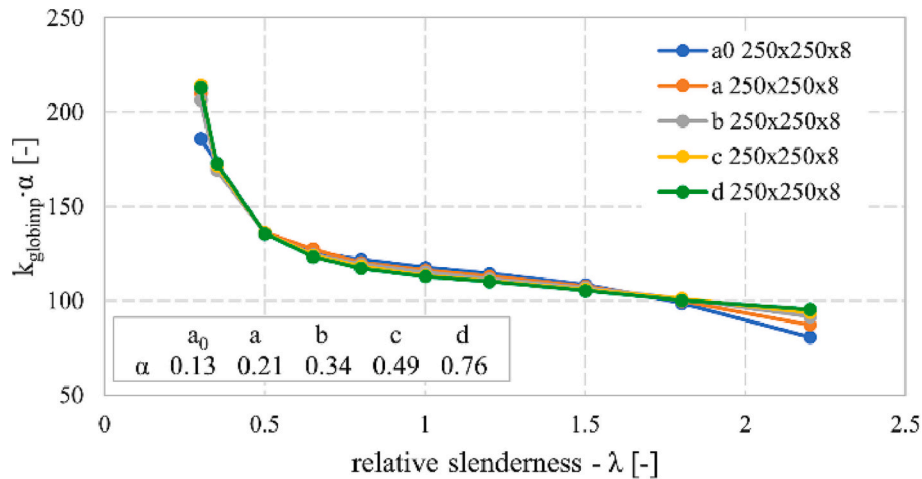
Fig. 5. Verification of numerical model (S960-120 × 6 – L = 1200 mm) [46].

**Table 2**  
Investigated cross-sections.

	yield strength	coefficient	width	height	thickness	b/t ratio	cross-section class
	$f_y$	$\varepsilon$	$b$	$h$	$t$	$b/t$	
	[Mpa]	[-]	[mm]	[mm]	[mm]	[-]	
Analysed cross-sections	355	0.8136	125	125	4	31.25	2
	355	0.8136	250	250	8	31.25	2
	355	0.8136	500	500	16	31.25	2
	355	0.8136	120	120	6	20.00	1
	355	0.8136	250	250	12	20.83	1
	355	0.8136	150	150	8	18.75	1
	355	0.8136	280	280	8	35.00	3



**Fig. 6.** Imperfection amplifiers required to recover the load carrying capacity corresponding to the standard buckling curves in the function of the relative slenderness.

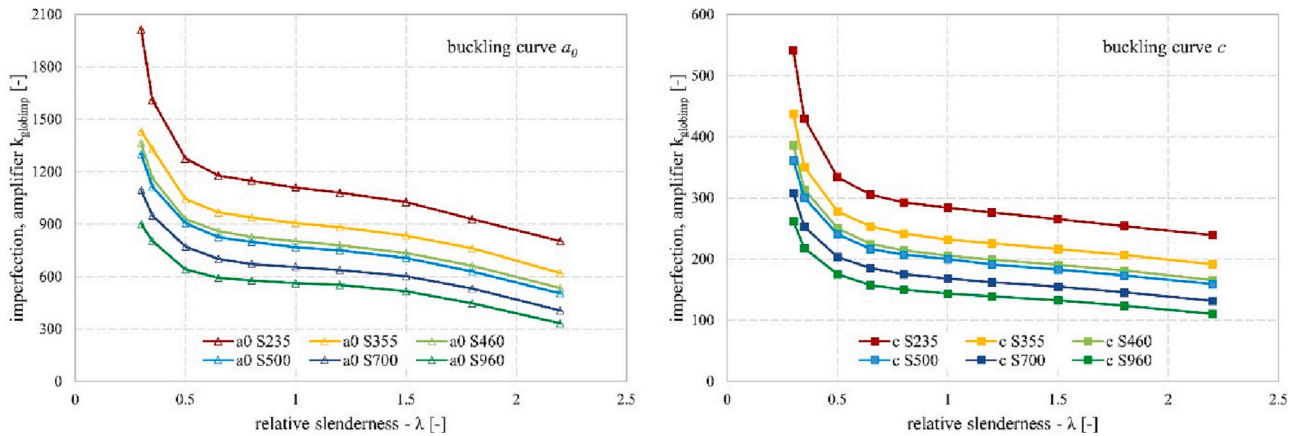


**Fig. 7.** Imperfection amplifier curves for a single section size multiplied by the imperfection factor  $\alpha$ .

**Table 3**

Investigated cross-sections for different steel grades.

	yield strength	coefficient	width	height	thickness	b/t ratio	cross-section class
	$f_y$	$\varepsilon$	$b$	$h$	$t$	$b/t$	
	[MPa]	[–]	[mm]	[mm]	[mm]	[–]	
Analysed steel grades	235	1.0000	250	250	8	31.250	1
	355	0.8136	250	250	8	31.25	2
	460	0.7148	250	250	8	31.250	3
	500	0.6856	240	240	8	30.000	3
	700	0.5794	200	200	8	25.000	3
	960	0.4948	175	175	8	21.875	3

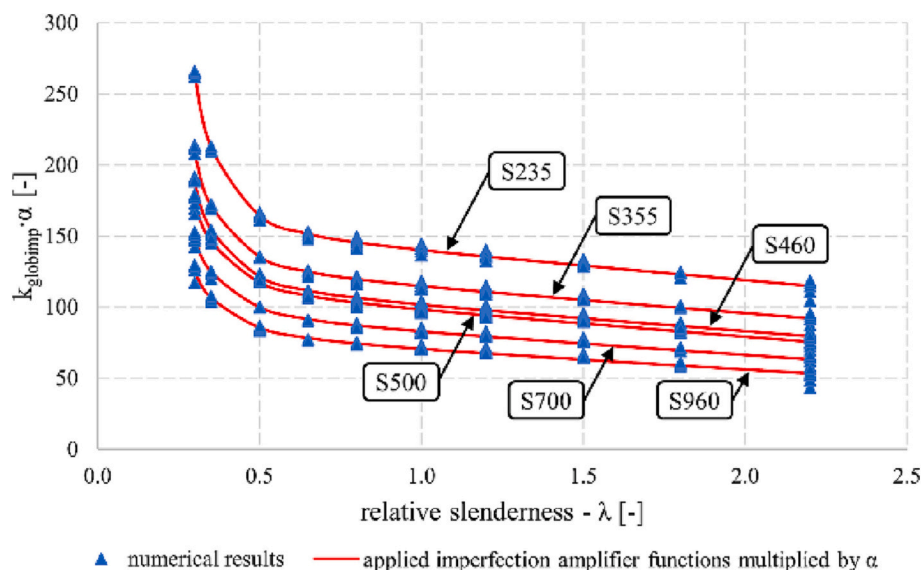
**Fig. 8.** Imperfection amplifiers required to recover the load carrying capacity values corresponding to the standard buckling curves  $a_0$  and  $c$  in the function of the relative slenderness (different steel grades).**Table 4**

Applicable constants to the imperfection amplifier formula for different steel grades.

	S235	S355	S460	S500	S700	S960
A	−3.90	−3.64	−3.57	−3.44	−3.32	−3.18
B	20.2	18.2	17.7	18.2	15.6	13.6
C	159	132	119	116	97.7	83.4

### 5.3. General approximate function

For practical usability, an approximate function is sought which, knowing the relative slenderness and steel grade, can be used to obtain generally the required equivalent geometric imperfection magnitudes. Based on the previous findings a general function, Eq. (7) is developed to provide the necessary equivalent geometric imperfection amplitudes in function of the slenderness, yield strength and imperfection factor  $\alpha$  of the desired buckling curve.

**Fig. 9.** Imperfection amplifiers multiplied by the imperfection factor  $\alpha$  for different steel grades.

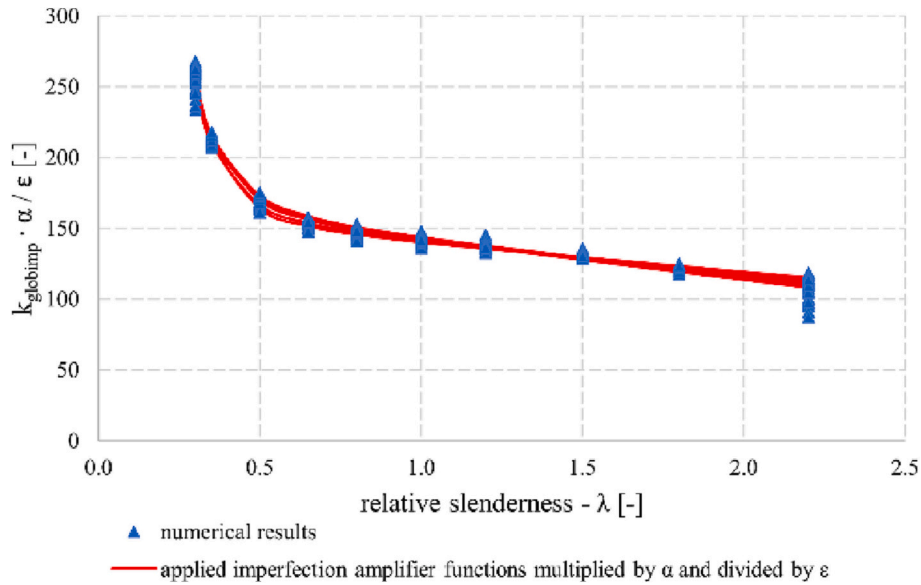


Fig. 10. Imperfection amplifier curves multiplied by the imperfection factor  $\alpha$  and divided by the coefficient  $\varepsilon$  for different steel grades.

$$k_{globimp} = \frac{\varepsilon}{\alpha} (\lambda_{rel}^{-3.8} - 26\lambda_{rel} + 168) \quad (7)$$

where  $\lambda$  is relative slenderness,  $\alpha$  is imperfection factor,  $\varepsilon$  is  $\sqrt{(235/f_y)}$ .

Fig. 11 plots together the numerically calculated results (blue dots), the unique approximate functions for each steel grades (red lines) and the general approximate function (black dashed line) as a function of relative slenderness. The comparison of the red and black lines shows a good agreement, which means that the general approximate function gives a good estimate of the required imperfection magnitude regardless of the actual steel grade, buckling curve, or relative slenderness.

#### 5.4. Validation and error of the general approximate function

GMNI analyses are performed using the imperfection amplifier obtained by the general approximation function for the columns having different steel grades presented in Table 3. It is investigated to what extent the load carrying capacity obtained from the numerical calculation differs from the result of the manual calculation according to

EN1993-1-1 [1]. The percentage of deviation (relative error) is calculated for each case according to Eq. (4), which resulted always  $<2\%$ . The mean of the relative error  $\delta$  for the whole data set (300 columns) is  $-0.009\%$ , the total root-mean-square (RMS) is  $0.48\%$ . Table 5 and Table 6 summarise the accuracy of the approximation function for the different buckling curves and steel grades, respectively. The approximation function gives the most accurate results for the buckling curve b, in which case the deviation is always  $<1\%$ .

Table 5  
Errors for different deflection curves.

	all results		$\lambda < 2.2$	
	abs. max. error [%]	RMS [%]	abs. max. error [%]	RMS [%]
a0	1.83%	0.45%	0.81%	0.26%
a	1.40%	0.34%	0.60%	0.23%
b	0.91%	0.28%	0.60%	0.25%
c	1.16%	0.43%	0.97%	0.39%
d	1.84%	0.77%	1.84%	0.67%

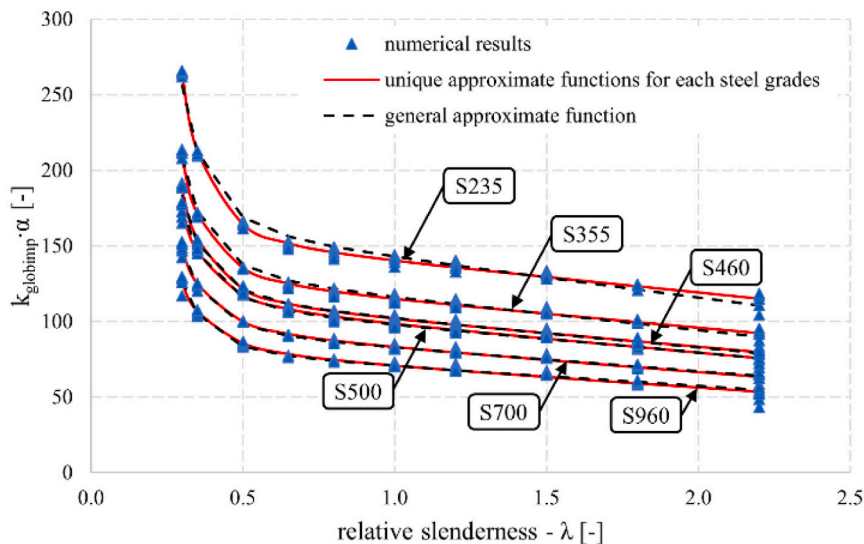


Fig. 11. General and unique approximate functions for each steel grades multiplied by the imperfection factor  $\alpha$ .



**Table 6**

Errors for different steel grades.

	all results	
	abs. max. error [%]	RMS [%]
S235	1.84%	0.66%
S355	1.57%	0.48%
S460	1.42%	0.40%
S500	1.37%	0.42%
S700	1.49%	0.43%
S960	1.83%	0.47%

The largest errors typically occur at a slenderness of 2.2. Therefore, the cases of relative slenderness  $\lambda < 2.2$  are also considered separately. It can be observed that for curves a<sub>0</sub>, a, b and c a better fit is observed over this range. Thus, excluding the corresponding results, all four curves show only deviations below 1%. But for curves d, the relative slenderness of 2.2 is not the most critical in terms of inaccuracy. Both the largest errors and the largest standard deviation are found for the buckling curve d. The errors according to the buckling curves are also illustrated in Fig. 12.

Also, the accuracy of the results obtained with the imperfection amplifier based on the general approximate function for different steel grades is investigated. The errors are summarised in Table 6. Not

considering results for relative slenderness to  $\lambda = 2.2$ , all but S235 and S355 material grades show deviations of  $< 1\%$ . The approximating function gives the largest errors in the load carrying capacity for steel grade S235.

To assess the given accuracies also the load carrying capacities are calculated using GMNI analysis applying the equivalent imperfection proposed by Walport et al. [9] according to Eq. (1). Fig. 13 shows the relative errors if the equivalent imperfection is used based on Eq. (1). In the figure, the darker colours indicate the higher steel grade. The results show that the error highly depends on the yield strength and in case of high yield strength the GMNI analysis can highly ( $> 10\%$ ) overpredict the resistance level of Eurocode if equivalent imperfection according to Walport et al. [9] is used. This can be explained by the fact that the target resistance for the creation of Eq. (1) was not the resistance level of Eurocode but a benchmark load capacity of GMNI analysis using L/1000 imperfection and residual stress. Table 7 compares the relative error  $\delta$  between the Walport function (Eq. (1)) and the newly proposed general equivalent imperfection function (Eq. (7)), the results show that for welded square box-sections the new function predicts the flexural buckling resistance of EN 1993-1-1 [1] much more accurately, however, its application is more complex. It should be noted, Walport's equation has been developed for standardization purposes and applicable more generally, therefore, it contains several simplifications, decreasing its

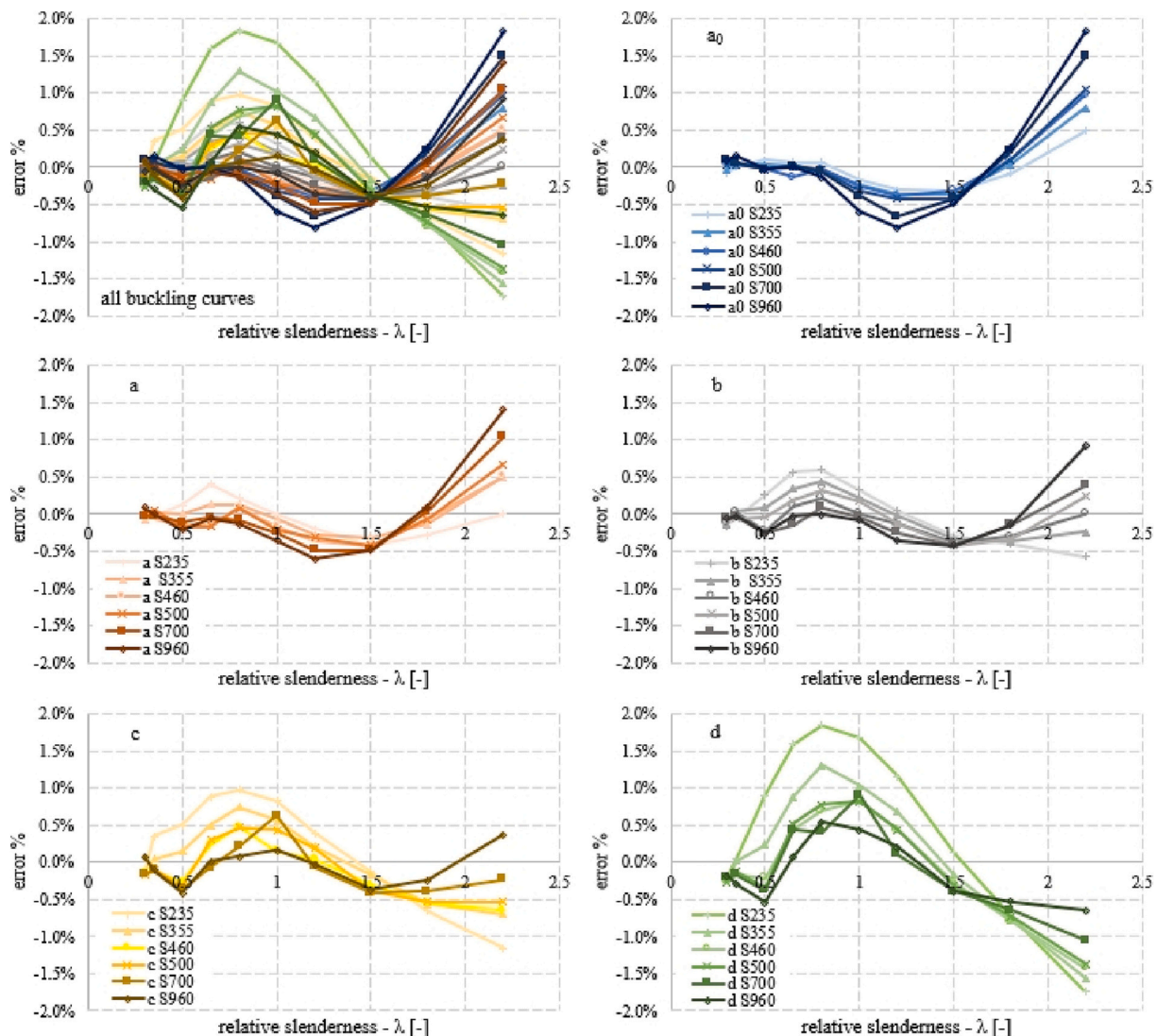


Fig. 12. Relative errors for load carrying capacity using the general approximation function for equivalent imperfection.

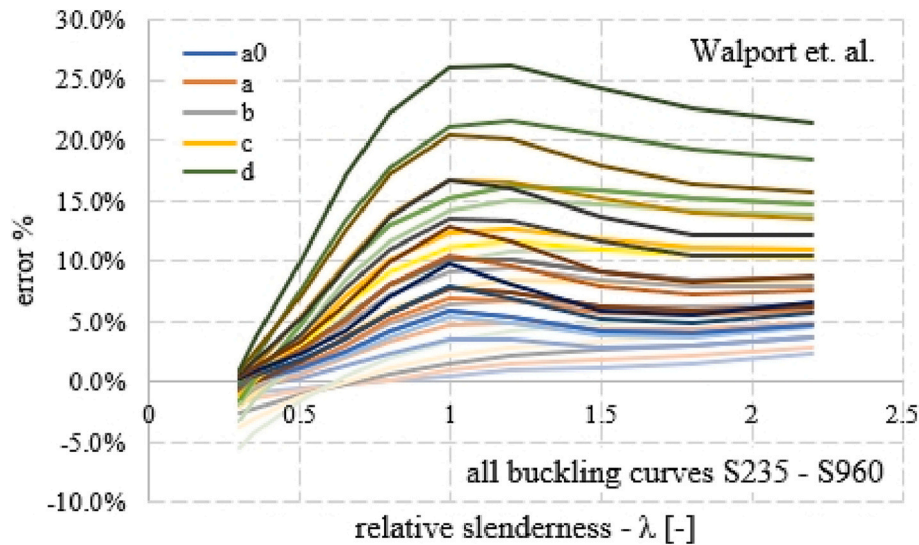


Fig. 13. Relative errors for load carrying capacity using Eq. (1) by Walport [9] for equivalent imperfection.

Table 7

Comparison of errors for proposed equivalent imperfection function and Walport [9] function.

relative error $\delta$ [%]	Walport et al.	new proposal
mean	6.04%	-0.01%
RMS	8.57%	0.48%
abs. max	26.2%	1.84%

accuracy.

#### 5.5. Statistical evaluation and determination of a constant amplitude imperfection

To derive a simplified approach for the application of the imperfection scaling factor (imperfection amplifier factor multiplied by the imperfection factor  $\alpha$  and divided by the coefficient  $\varepsilon$ ), the determined imperfection amplifiers are statistically evaluated. The maximum, minimum, average and RMS values of the obtained data points are determined and introduced in Table 8. The mean value of the general approximate function is also determined using Eq. (8).

$$f_{\text{mean}} = \frac{\int_a^b f(x)}{b-a} \quad (8)$$

The  $[a, b]$  range of integration is chosen  $[0.3, 2.2]$ , which is a commonly used parameter range within the daily design praxis and  $f(x)$  is the derived general approximation function having the variable of the relative slenderness. While the mean of the results depends on the distribution of the relative slenderness ratio, the mean of the function gives the relevant result. Fig. 14 illustrates the difference between the two calculated mean values.

Table 8

Statistical evaluation of the imperfection scaling factor and the mean value of the general approximation function.

	max.	min.	RMS	mean of results	average of app. function
Imperfection scaling factor ( $k_{\text{globimp}} \cdot \alpha/\varepsilon$ ) for square cross-section	298.48	87.36	43.12	158.71	140.95

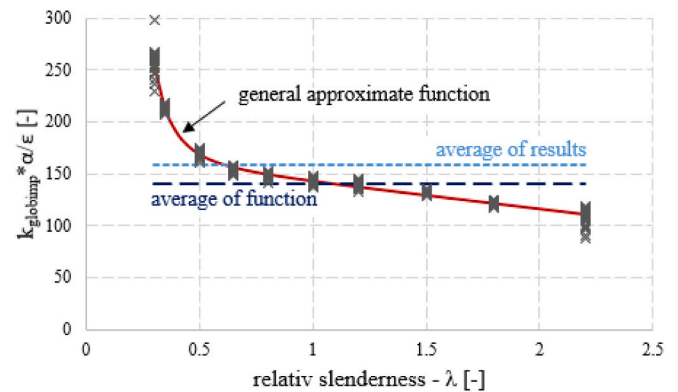


Fig. 14. Average of the imperfection amplifier results multiplied by the imperfection factor  $\alpha$  and divided by the coefficient  $\varepsilon$ , and the mean of general approximation function.

## 6. Investigation of rounded section

### 6.1. Description of the analysed columns

The cross-section geometry of square sections may vary depending on the manufacturing process. In civil engineering practice usually three main types exist; welded, hot-rolled and cold-formed. For the latter two, corners of the cross-section are rounded. In this chapter, the effect of the rounded corner is examined. For the sake of simplicity, hot-rolled and cold-formed sections are examined together and will be referred to as rounded sections. Of course, the real buckling behaviour of a hot-rolled and cold-formed column could be different because the residual stresses differ, but in present research equivalent geometric imperfections are applied, where the residual stress is only taken into consideration through the selection of the appropriate buckling curve. In our research all the buckling curves are evaluated, therefore the results derived based on a simple rounded section could be applied for cold-formed and hot-rolled sections as well. Welded sections are examined in the previous chapters, in this chapter it is also investigated whether the same function can be used for rounded sections. The numerical model remains essentially the same with only the cross-section varying. Since in practice the radius of curvature is generally about  $r_{\text{out}} = 2 \text{ t} - 3 \text{ t}$ , a radius of curvature of one kind is used. Fig. 15 shows the rounded cross-section. In the numerical model the corner region is modelled using one finite element,

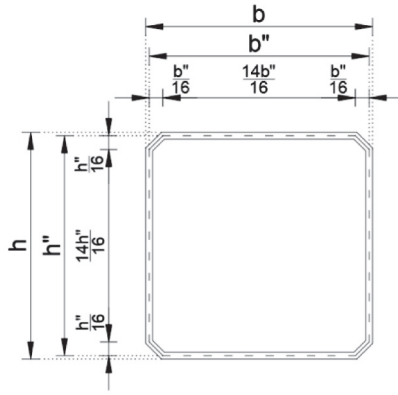


Fig. 15. Rounded section in numerical model.

because using this strategy the mesh size in the corner region is about the same as in the flat parts. Following this strategy, it is calculated what is the corresponding radius of curvature based on the equality of the area of cross-section, this is represented by Eq. (9). Based on this it is found that the applied outer radius of curvature is about  $r_{out} = 2 \text{ t} - 3 \text{ t}$  for all the examined cross-sections depending on the exact geometry. The same six steel grades were used as before, and the cross-sectional dimensions again chosen so that the cross-sectional class is 3 or less (see Table 3, now the dimensions  $h$  and  $b$  are the sides of the enclosing square).

$$r_{out, corresponding} = \left( \frac{b}{t} - 1 \right) \frac{2 - \sqrt{2}}{8(4 - \pi)} + \frac{1}{2} \quad (9)$$

## 6.2. Accuracy of the general approximating function for rounded square box section

Calculated with the  $k_{globimp}$  values taken from the general approximation function (Eq. (7)) larger errors in load capacity are observed, but in this case, the differences are still <3% in all cases. The general results of comparing the errors associated with the use of the approximation function for rounded and welded girders are shown in Table 9 (2nd and 3rd columns).

In this case, it is also observed both the largest value and the largest standard deviation of the relative error are at a relative slenderness value of 2.2. The relative error of the load carrying capacities obtained by applying the equivalent geometric imperfections from the general approximation formula is shown in Fig. 16 (a). In the figures, the darker colours indicate the higher steel grade.

## 6.3. Modification of the general approximation function for rounded box sections

For higher relative slenderness, more significant differences are observed, so if a more accurate result is required, the general approximation function given by Eq. (6) is modified by an additional formula ( $\beta_{mod}$ ), which is only applicable if  $\lambda_{rel} \geq 1$ . This modified approximation function for rounded square sections is defined by Eqs. (10)–(11).

$$k_{globimp} = \frac{\varepsilon}{\alpha} (\lambda_{rel}^{-3.8} - 26\lambda_{rel} + 168 + \beta_{mod}) \quad (10)$$

Table 9  
Comparison of errors for welded and rounded girders.

errors [%]	welded section	rounded section	rounded section 2*
mean	−0.01%	−0.43%	0.001%
RMS	0.48%	0.73%	0.48%
abs. max.	1.84%	2.47%	1.84%

\* Using the modified function (see chapter 6.3)

where:

$$\beta_{mod} = -15\lambda_{rel}^2 + 50\lambda_{rel} - 32 \text{ if } \lambda_{rel} \geq 1.0 \quad (11)$$

Using the modified formula for the rounded section, thus essentially the same accuracy can be achieved for welded section and rounded section, as shown in the last column of Table 9 (“rounded section 2”). Fig. 17 shows the two approximation functions and the numerical results. It can be observed the general approximation function always provides slightly lower imperfection amplifier, therefore results in lower buckling resistance than the accurate modified function. This means that the application of the general approximation function gives a safe-side approximation for the buckling resistance of rounded square sections.

## 6.4. Statistical evaluation and simplification

The obtained imperfection scaling factors (amplifiers multiplied by the imperfection factor  $\alpha$  and divided by the  $\varepsilon$ ) are statistically evaluated in the case of cold-formed sections as well. The maximum, minimum, average and RMS values are determined, see Table 10. As described in Section 5.5, the mean of the modified function is also calculated according to Eq. (8).

## 7. Investigation of rectangular sections

### 7.1. Description of the analysed columns

Rectangular box-sections are also studied over a wide range of  $b/h$  ratio. For rectangular sections only S355 steel grade is examined. The numerical model differs from the previous ones only in the geometry of the cross-section. When choosing the cross-section dimensions, cross-section class 4 sections are still avoided. The parameters of the tested sections are given in Table 11.

### 7.2. Accuracy of the general approximating function for rectangular box section

Calculated with the equivalent geometric imperfections from the general approximation function, the larger the  $b/h$  ratio of the section under consideration, the larger the error in the load carrying capacity. Even for the smallest tested  $b/h$  ratio, a maximum error of >2% is obtained, which is larger than for the welded square box-section. The results show that, in contrast to the rounded square section, the application of the general approximation function produces in many cases higher resistance than the target resistance, thus in some cases producing an error of 2–3% at the expense of safety. Therefore, a modification factor is needed to cover the load carrying capacity more accurately. The exact errors for the different sections are summarised in Table 12 and Fig. 18.

### 7.3. Modification of the general approximation function for rectangular box-sections

The necessary equivalent imperfections are calculated for the examined rectangular sections using the procedure described in Section 3. The numerical results show the required equivalent geometric imperfection is dependent on the  $b/h$  ratio. Fig. 19 shows the required equivalent geometric imperfections as a function of relative slenderness.

Fig. 20 represents the same results multiplied by the imperfection parameter  $\alpha$ , it shows that unlike for the square section, multiplication by  $\alpha$  does not bring the results for the different imperfection curves into line in case of higher aspect ratios. It is also clear that the discrepancies in this respect also increase as the  $b/h$  ratio increases. Results show that if aspect ratio  $b/h$  equal to 3 or lower then imperfection amplifier depends linearly on the imperfection factor  $\alpha$ , as in the case of square sections, therefore for these cases the general approximation

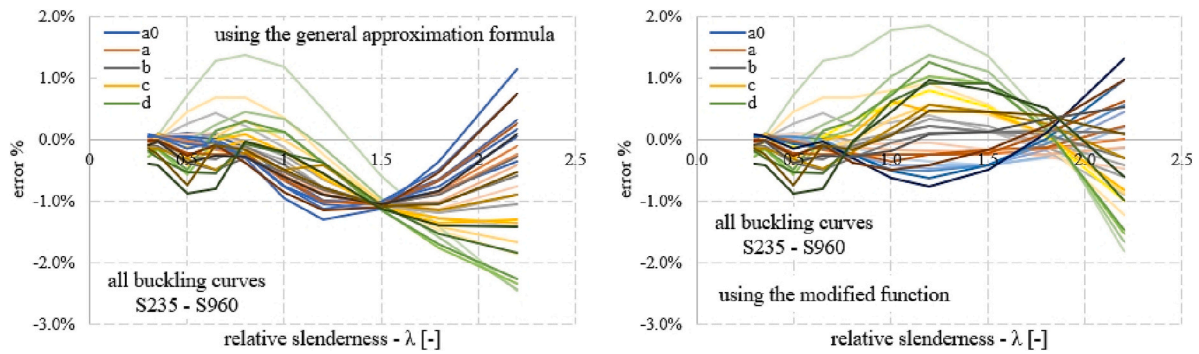


Fig. 16. Relative error in load carrying capacity calculated using the general approximation formula (a) and using the modified function (b) - (see chapter 6.3).

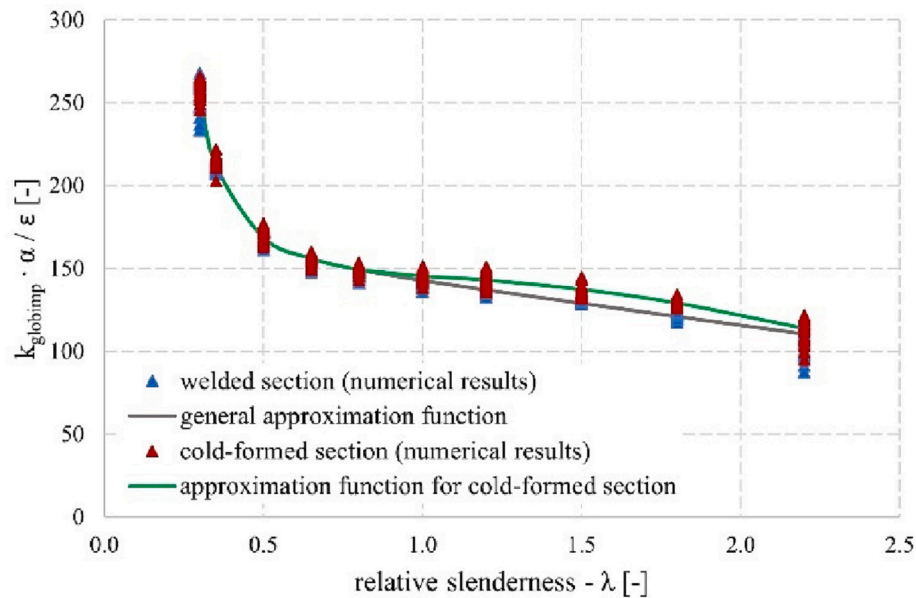


Fig. 17. Approximation function for rounded section.

Table 10

Statistical evaluation of the imperfection scaling factor, and the mean value of the modified approximation function.

	max.	min.	RMS	mean of results	average of app. function
Imperfection scaling factor ( $k_{globimp} \cdot \alpha / \epsilon$ ) for cold-formed section	265.88	94.72	41.25	161.83	145.88

Table 11

Investigated rectangular box sections.

	yield strength	Coefficient	b/h ratio	height	width	thickness	b/t ratio	cross-section class
	$f_y$	$\epsilon$	b/h	h	b	t	b/t	
	[MPa]	[-]	[-]	[mm]	[mm]	[mm]	[-]	
Analysed cross-sections	355	0.814	1.25	240	300	10	30.00	2
	355	0.814	1.50	200	300	10	30.00	2
	355	0.814	2.00	150	300	8	37.50	2
	355	0.814	3.00	100	300	8	37.50	2
	355	0.814	4.00	100	400	8	50.00	3
	355	0.814	5.00	100	500	8	62.50	2

function can be applied with a slight modification. However, for aspect ratio  $b/h$  equal to 4 or 5 there are too big differences, and imperfection amplifier  $k_{globimp}$  depends differently on imperfection factor  $\alpha$  than that

Table 12

Errors in load carrying capacity using the general approximation function for rectangular box sections with different  $b/h$  ratios.

b/h	1.25	1.5	2	3	4	5
Mean	0.31%	0.43%	0.54%	0.44%	0.16%	-0.32%
abs. max	2.07%	2.38%	2.76%	3.14%	2.93%	2.45%
RMS	0.69%	0.81%	0.97%	1.08%	1.12%	1.35%



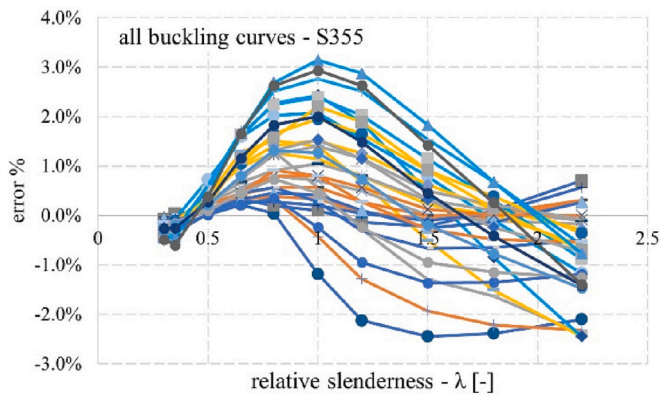


Fig. 18. Relative errors in load carrying capacity using the general approximation function for rectangular box sections in function of slenderness.

is suggested by the general approximation function. Therefore, for rectangular sections with high  $b/h$  ratios further research is needed, and the below suggested equivalent imperfection function is applicable only if  $b/h$  aspect ratio is not higher than 3.

For rectangular sections if aspect ratio  $b/h$  is smaller or equal than 3 a modified version of the general approximation function can predict accurately the applicable equivalent imperfection. But for small slenderness, no modification of the general approximation formula is necessary. If the relative slenderness is greater or equal than 0.5, it is suggested to add a factor  $\gamma_{mod}$  depending on the relative slenderness to the original formula according to Eqs. (12)–(13).

$$k_{globimp} = \frac{\varepsilon}{\alpha} (\lambda_{rel}^{-3.8} - 26\lambda_{rel} + 168 + \gamma_{mod}) \quad (12)$$

where:

$$\gamma_{mod} = 3.5\lambda_{rel} - 8 \text{ if } \lambda_{rel} \geq 0.5 \quad (13)$$

With this modification, for rectangular sections with a ratio of 1.25–2  $b/h$ , approximately the same accuracy can be achieved as for square box-sections as described earlier. In all cases, the maximum absolute error is  $<2\%$  for the load carrying capacity. If the  $b/h$  ratio is 3, the maximum absolute deviation exceeds 2%, and for higher  $b/h$  ratios further refinement is needed. Fig. 21 and Table 13 summarise the errors for  $b/h = 1.25..0.3$  using the modified formula.

#### 7.4. Statistical evaluation and simplification

The imperfection scaling factors (amplifiers multiplied by the imperfection factor  $\alpha$  and divided by the  $\varepsilon$ ) are statistically evaluated in the case of rectangular sections as well. The maximum, minimum, average and RMS values are determined and given in Table 14.

The mean value of the developed function is also determined as described in Section 5.5, according to Eq. (8). The calculated average values are shown in Fig. 22.

## 8. Conclusions

In the present study, a numerical analysis is performed to determine the required equivalent geometric imperfection to be used in GMNI analysis to give the same flexural buckling resistance as the manual calculation using the buckling curves prescribed by EN1993-1-1 [1]. Square and rectangular box-section columns subjected to concentrated compressive forces are tested. The study covers welded, cold-formed and hot-rolled square sections and welded rectangular sections. Several steel grades are examined ranging from S235 up to S960. Based on the numerical study the following conclusions are drawn:

- The dimensions and proportions of the square box-section (width, thickness,  $b/t$  ratio) do not affect the required equivalent geometric imperfection.
- The magnitude of the required equivalent geometrical imperfection is determined for five buckling curves. A fitted analytical function is

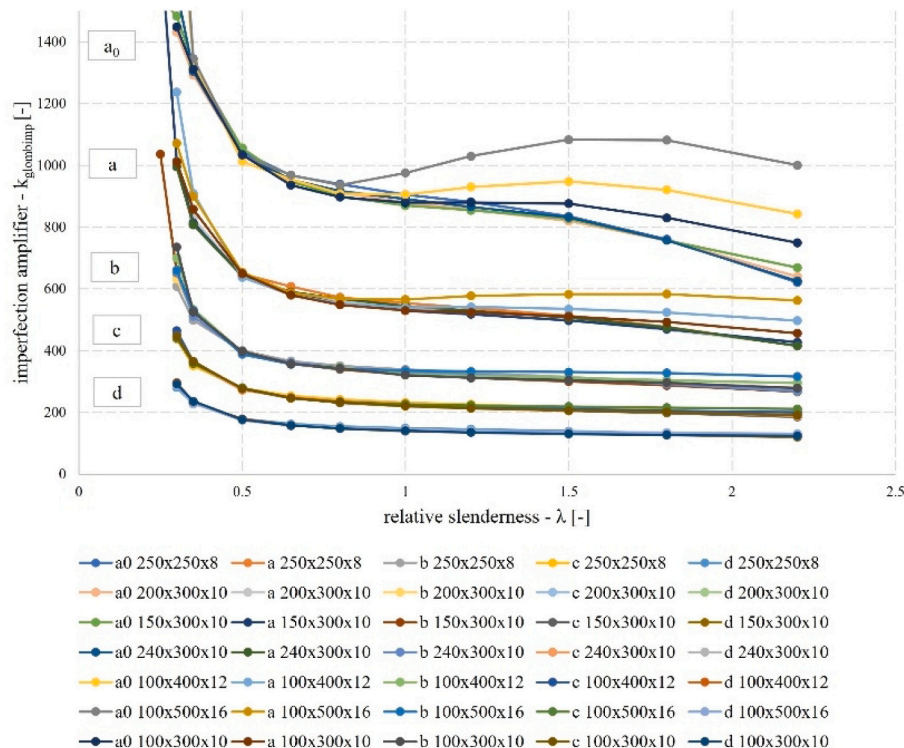


Fig. 19. Required equivalent geometric imperfections.

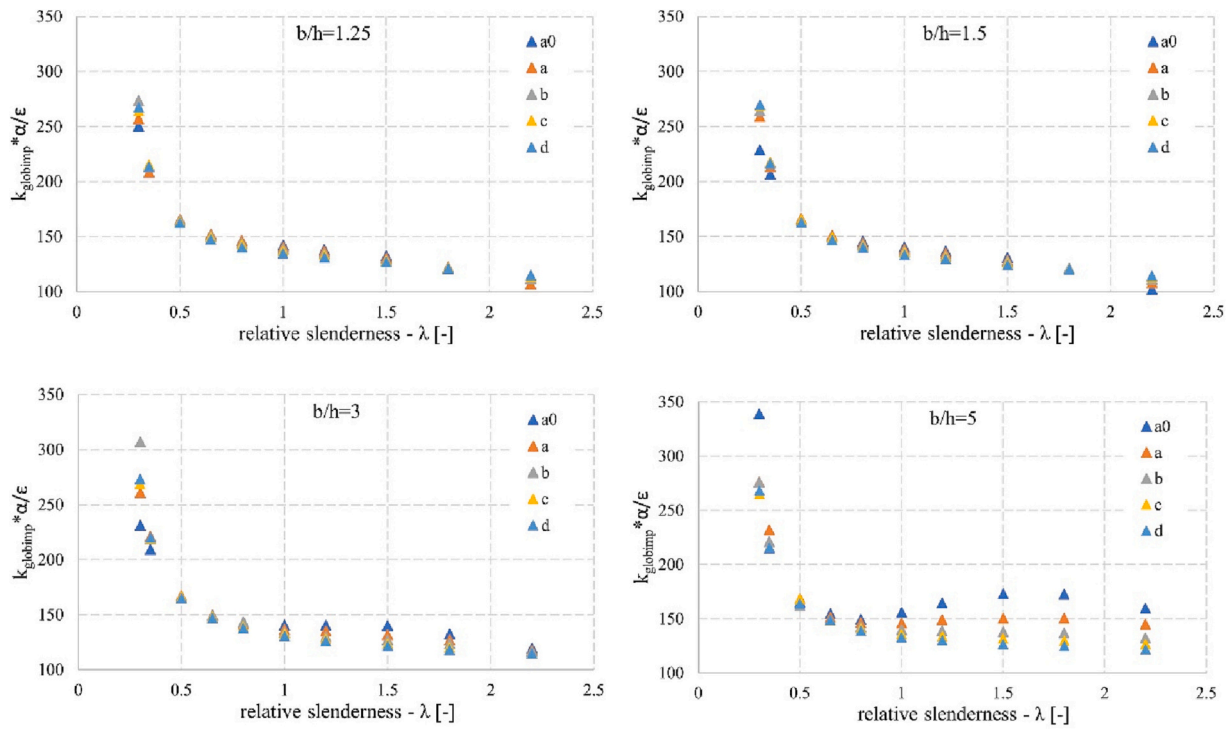


Fig. 20. Required imperfection magnitudes multiplied by alpha parameter divided by  $\epsilon$ .

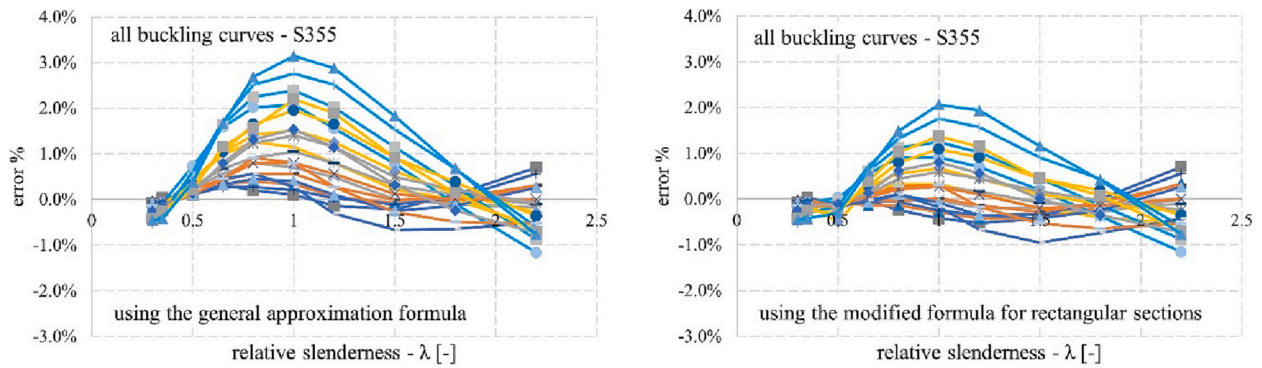


Fig. 21. Relative error in load carrying capacity for rectangular sections ( $b/h \leq 3$ ) calculated using the general approximation formula (a) and using the modified function – Eqs. (12)–(13) (b).

Table 13

Errors in load carrying capacity using the modified function (Eqs. (12)–(13)) for rectangular box-sections with different  $b/h$  ratios.

$b/h$	1.25	1.5	2	3
Mean	−0.06%	0.05%	0.15%	0.08%
abs. max	1.15%	1.25%	1.76%	2.06%
RMS	0.37%	0.40%	0.54%	0.70%

Table 14

Statistical evaluation of the imperfection scaling factor, and the mean value of the modified approximation function in the case of rectangular sections.

	max.	min.	RMS	mean of results	average of app. function
Imperfection scaling factor ( $k_{globimp} \cdot \alpha / \epsilon$ ) for rectangular section	242.64	99.96	28.52	149.02	138.02

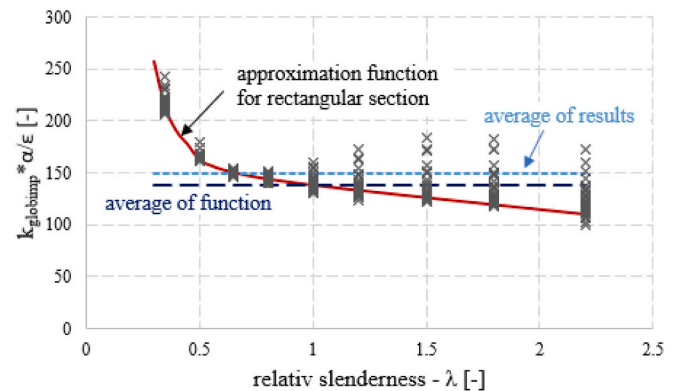


Fig. 22. Average of the imperfection amplifier results multiplied by the imperfection factor  $\alpha$  and divided by the coefficient  $\epsilon$ , and of the modified approximation function for rectangular sections.

given by Eq. (14) depending on the relative slenderness ratio and steel grade for welded square box-section columns to predict the applicable equivalent geometrical imperfection magnitude.

$$k_{globimp} = \frac{\varepsilon}{\alpha} (\lambda_{rel}^{-3.8} - 26\lambda_{rel} + 168) \quad (14)$$

- Using the imperfection obtained by applying the general approximation function for welded square box-sections, the load carrying capacity obtained from the GMNIA results differs in all cases by <2% from the load carrying capacity obtained by manual calculation according to EN1993-1-1 [1].
- For rounded square box-sections (hot-rolled, cold-formed), it is recommended to add a modifier to the general approximation function depending on the relative slenderness. Using this modified formula, again an error of <2% in the load capacity is obtained for this type of section.

$$k_{globimp,rounded} = \frac{\varepsilon}{\alpha} (\lambda_{rel}^{-3.8} - 26\lambda_{rel} + 168)$$

$$\text{if } \lambda_{rel} < 1.0 \quad k_{globimp,rounded} = \frac{\varepsilon}{\alpha} (\lambda_{rel}^{-3.8} - 15\lambda_{rel}^2 + 24\lambda_{rel} + 136) \quad \text{if } \lambda_{rel} \geq 1.0 \quad (15)$$

- Rectangular box-sections are also tested for S355 steel grade, with the b/h ratio varying from 1.25 to 5. The geometry of the rectangular box section (b/h ratio, thickness) influences the required equivalent geometric imperfection. By using the general approximation formula, larger deviations are observed compared to the load carrying capacity calculated according to EN1993-1-1 [1]. Multiplication by imperfection factor  $\alpha$  does not bring the required equivalent geometric imperfection curves for the different deflection curves into alignment as for square sections if aspect ratio b/h is higher than 3. By modifying the original function if aspect ratio b/h < 3, a maximum error of 2% in the load carrying capacity is obtained.

$$k_{globimp,rect,S355} = \frac{\varepsilon}{\alpha} (\lambda_{rel}^{-3.8} - 26\lambda_{rel} + 168)$$

$$\text{if } \lambda_{rel} < 0.5 \quad k_{globimp,rect,S355} = \frac{\varepsilon}{\alpha} (\lambda_{rel}^{-3.8} - 22.5\lambda_{rel} + 160) \quad \text{if } \lambda_{rel} \geq 0.5 \quad (16)$$

- Based on the executed statistical evaluation, a simplified equation is determined based on the average imperfection scaling factor providing sufficient average safety for the buckling resistance calculation; the simplified scaling factor is independent of the relative slenderness ratio and cross-section geometries, given by Eq. (17).

$$k_{globimp,general} = 150 \frac{\varepsilon}{\alpha} \quad (17)$$

#### CRedit authorship contribution statement

**B. Somodi:** Methodology, Software, Validation, Data curation, Writing – review & editing, Project administration. **E. Bärnkopf:** Methodology, Software, Validation, Writing – original draft, Visualization. **B. Kövesdi:** Conceptualization, Writing – review & editing, Supervision.

#### Declaration of Competing Interest

The authors declare the following financial interests/personal relationships which may be considered as potential competing interests:

Dr. Balazs Somodi reports financial support was provided by

Hungarian Academy of Sciences. Dr. Balazs Kovésvi reports financial support was provided by Hungarian Academy of Sciences.

#### Data availability

Data will be made available on request.

#### Acknowledgements

The presented research program has been financially supported by the Grant MTA-BME Lendület LP2021-06 / 2021 "Theory of new generation steel bridges" program of the Hungarian Academy of Sciences, which is gratefully acknowledged.

#### References

- [1] EN 1993-1-1, Eurocode 3: Design of steel structures - Part 1.1: General rules and rules for buildings, 2005.
- [2] R.D. Ziemian, Advanced methods of inelastic analysis in the limit states design of steel structures, Cornell University, 1990, 1990.
- [3] R.D. Ziemian, W. McGuire, G. Deierlein, Inelastic limit states design. Part 1: planar frame studies, J. Struct. Eng. ASCE 118 (1992) 2532–2549.
- [4] S.L. Chan, W.F. Chen, Advanced analysis as a new dimension for structural steel design, Adv. Steel Constr. 1 (2005) 87–102.
- [5] S.G. Buonopane, B.W. Schafer, Reliability of steel frames designed with advanced analysis, J. Struct. Eng. 132 (2006) 267–276.
- [6] H. Zhang, S. Shayan, K.J.R. Rasmussen, B.R. Ellingwood, System-based design of planar steel frames, I: reliability framework, J. Constr. Steel Res. 123 (2016) 135–143.
- [7] A. Fieber, L. Gardner, L. Macorini, Design of structural steel members by advanced inelastic analysis with strain limits, Eng. Struct. 199 (2019), 109624.
- [8] L. Gardner, X. Yun, A. Fieber, L. Macorini, Steel design by advanced analysis: material modeling and strain limits, Engineering 5 (2019) 243–249.
- [9] F. Walport, L. Gardner, D.A. Nethercot, Equivalent bow imperfections for use in design by second order inelastic analysis, Structures 26 (2020) 670–685.
- [10] B. Somodi, B. Kövesdi, Residual stress measurements on welded square box sections using steel grades of S235–S960, Thin-Walled Struct. 123 (2018) 142–154, <https://doi.org/10.1016/j.tws.2017.11.028>.
- [11] B. Somodi, B. Kövesdi, Residual stress measurements on cold-formed HSS hollow section columns, J. Constr. Steel Res. 128 (2017) 706–720.
- [12] EN 1993-1-5, Eurocode 3: Design of steel structures - Part 1.5: Plated structural elements, 2005.
- [13] EN 1090-2, EN 1090-2 - Execution of steel structures and aluminium structures. Part 2: Technical requirements for steel structures, BSI, 2018, 2018.
- [14] W.E. Ayrton, J. Perry, On Struts, The Engineer, 1886. Dec. 10, pp. 464–465.
- [15] W.E. Ayrton, J. Perry, On Struts, The Engineer, 1886. Dec. 24, pp. 513–515.
- [16] A. Taras, R. Greiner, New design curves for lateral-torsional buckling – proposal based on a consistent derivation, J. Constr. Steel Res. 66 (2010) 648–663.
- [17] D. Sfintesco (Ed.), ECCS European Recommendations for Steel Construction, European Convention for Constructional Steelwork, Brussels, 1978.
- [18] D. Sfintesco, A. Carpena, Experimental Bases of the ECCS Column Curves, 2nd Intern. Coll. on Stability Introductory Report, Tokyo, (Liege, Washington), 1977, pp. 68–75.
- [19] J. Jacquet, Essais de Flambement et Exploitation Statistique, Construction Métallique 3, 1970, pp. 14–36.
- [20] S. Strating, H. Vos, Computer simulation of the ECCS buckling curve using a Monte-Carlo method, in: Proc. of the International Colloquium on Column Strength, 1972.
- [21] H. Beer, G. Schulz, Bases théoriques des courbes européennes de flambement, Construction Métallique 3 (1970) 5–12.
- [22] R. Maquoi, J. Rondal, Mise en équation des nouvelles courbes européennes de flambement, Construction Métallique 1 (1978) 17–30.
- [23] J. Rondal, R. Maquoi, Formulation d'Ayrton-Perry pour le flambement des barres métalliques, Construction Métallique 4 (1979) 41–53.
- [24] prEN 1993-1-1, Eurocode 3 – Design of steel structures – Part 1–1: General rules and rules for buildings. 2019, 2019.
- [25] S.L. Chan, H.Y. Huang, L.X. Fang, Advanced analysis of imperfect portal frames with semirigid base connections, J. Eng. Mech. (ASCE) 131 (6) (2005) 633–640.
- [26] S.E. Kim, Practical Advanced Analysis for Steel Frame Design, Ph.D. Thesis, Purdue University, West Lafayette, IN, 1996.
- [27] M. Kucukler, L. Gardner, L. Macorini, A stiffness reduction method for the in-plane design of structural steel elements, Eng. Struct. 73 (2014) 72–84.
- [28] I. González-de-León, I. Arrayago, E. Real, E. Mirambell, A stiffness reduction method for the in-plane design of stainless steel members and frames according to EN 1993-1-4, Eng. Struct. 253 (2022) 113740, <https://doi.org/10.1016/j.engstruct.2021.113740>.
- [29] American Institute of Steel Construction (ANSI/AISC), AISC 360. Specification for Structural Steel Buildings. Illinois, USA, 2016.
- [30] American Institute of Steel Construction (ANSI/AISC), AISC 370. Specification for Structural Stainless Steel Buildings. Illinois, USA, 2021.

- [31] Working Group 22 for Eurocode 3 CEN/TC 250/SC3/WG22, prEN 1993-1-14, Eurocode 3: Design of Steel Structures – Part 1–14: Design Assisted by Finite Element Analysis. Final Document. Brussels, Belgium, 2021.
- [32] AS 4100 Steel Structures, Standards Australia, Sydney, Australia, 2020.
- [33] AS/NZS 4600 Cold-Formed Structures, Standards Australia, Sydney, Australia, 2018.
- [34] European Committee for Standardization (CEN), prEN 1993-1-1, Eurocode 3: Design of Steel Structures – Part 1–1: General Rules and Rules for Buildings. Final Document. Brussels, Belgium, 2019.
- [35] S. Shayan, K.J.R. Rasmussen, H. Zhang, On the modelling of initial geometric imperfections of steel frames in advanced analysis, *J. Constr. Steel Res.* 98 (2014) 167–177.
- [36] J. Lindner, U. Kuhlmann, A. Just, Verification of flexural buckling according to Eurocode 3 part 1–1 using bow imperfections, *Steel Construct.* 9 (2016) 349–362.
- [37] J. Lindner, U. Kuhlmann, F. Jorg, Initial bow imperfections  $e_0$  for the verification of flexural buckling according to Eurocode 3 part 1–1 – additional considerations, *Steel Construct.* 11 (2018) 30–41.
- [38] EN 1990, Eurocode: Basis of structural design, 2023.
- [39] ANSYS® v19.2, Canonsburg, Pennsylvania, USA, 2023.
- [40] X. Yun, L. Gardner, Stress-strain curves for hot-rolled steels, *J. Constr. Steel Res.* 133 (2017) 36–46.
- [41] B. Somodi, B. Kövesdi, T. Hornyák, Partial factor for local buckling of welded box sections, *Structures* 30 (2021) 440–454.
- [42] T. Li, G. Li, S. Chan, Y. Wang, Behavior of Q690 high-strength steel columns: part 1: experimental investigation, *J. Constr. Steel Res.* 123 (2016) 18–30.
- [43] X. Qiang, F.S.K. Bijlaard, H. Kolstein, Post-fire performance of very high strength steel S960, *J. Constr. Steel Res.* 80 (2013) 235–242.
- [44] J. Wang, S. Afshan, N. Schillo, M. Theofanous, M. Feldmann, L. Gardner, Material properties and compressive local buckling response of high strength steel square and rectangular hollow sections, *Eng. Struct.* 130 (2017) 297–315.
- [45] X. Meng, L. Gardner, Testing of hot-finished high strength steel SHS and RHS under combined compression and bending, *Thin-Walled Struct.* 148 (2020), 106262.
- [46] B. Somodi, B. Kövesdi, Flexural buckling resistance of welded HSS box section members, *Thin-Walled Struct.* 119 (2017) 266–281.